

# Matrix Isolation Infrared Spectroscopic and Density Functional Theoretical Studies on the Reactions of Lanthanum Atoms with Acetylene

Yun-Lei Teng and Qiang Xu\*

National Institute of Advanced Industrial Science and Technology (AIST), Ikeda, Osaka 563-8577, Japan, and Graduate School of Engineering, Kobe University, Nada Ku, Kobe, Hyogo 657-8501, Japan

Received: May 14, 2008; Revised Manuscript Received: August 14, 2008

Laser-ablated lanthanum atoms have been codeposited at 4 K with acetylene in excess argon. Products,  $\text{La}(\text{C}_2\text{H}_2)$ ,  $\text{LaCCH}_2$ ,  $\text{HLaCCH}$ , and  $\text{La}_2(\text{C}_2\text{H}_2)$ , have been formed in the present experiments and characterized using infrared spectroscopy on the basis of the results of the isotopic shifts, mixed isotopic splitting patterns, stepwise annealing, the change of reagent concentration and laser energy, and the comparison with theoretical predictions. Density functional theory calculations have been performed on these molecules. The agreement between the experimental and calculated vibrational frequencies, relative absorption intensities, and isotopic shifts supports the identification of these molecules from the matrix infrared spectra. Plausible reaction mechanisms have been proposed to account for the formation of these molecules.

## Introduction

Considerable attention has been paid to the interactions of metal atoms with acetylene due to the industrial importance of hydrocarbon hydrogenation and dehydrogenation processes.<sup>1–3</sup> The interactions of metal atoms with acetylene have been investigated using the matrix isolation technique, and four bonding models, side-on  $\text{M}-\eta^2-(\text{C}_2\text{H}_2)$  (Cu, Ag, Au, Cr, Ni, Al, Pt, Pd, Li, U, Th), vinyl form  $\text{M}-\text{C}_2\text{H}_2$  (Al, Au), inserted  $\text{HMCCCH}$  (Be, B, Cr, Pt, Al, Fe, Cr), and vinylidene  $\text{M}=\text{C}=\text{CH}_2$  (Ni, Au, Pt, Na) have been identified and characterized by infrared and electron spin resonance spectroscopies.<sup>4–17</sup> In addition, kinds of products,  $\text{M}(\text{C}_2\text{H}_2)_2$  (Pd, U, Th),  $\text{MCCH}$  (Mg, U, Th), and  $\text{Pd}_2(\text{C}_2\text{H}_2)$ , have also been identified and characterized through the matrix isolation technique.<sup>11,17,18</sup> The interactions of metal with acetylene have also been extensively investigated by quantum chemical computations;<sup>18–23</sup> for example, the bonding of  $\text{La}^+$  and  $\text{La}^{2+}$  to  $\text{C}_2\text{H}_2$  has been investigated using the modified coupled pair functional method.<sup>21</sup> However, the reactions of La atoms with  $\text{C}_2\text{H}_2$  have not been investigated using the matrix isolation techniques and quantum chemical computations.

Recent studies have shown that, with the aid of isotopic substitution techniques, matrix isolation infrared spectroscopy combined with quantum chemical calculations is very powerful for investigating structure and bonding of novel species.<sup>14–17,24,25</sup> To understand the interaction of acetylene and lanthanum atoms, the reactions of laser-ablated lanthanum atoms with acetylene in a solid-argon matrix have been performed. IR spectroscopy and theoretical calculations provide evidence for the formation of products,  $\text{La}(\text{C}_2\text{H}_2)$ ,  $\text{HLaCCH}$ ,  $\text{LaCCH}_2$ , and  $\text{La}_2(\text{C}_2\text{H}_2)$ . The side-on  $\text{La}(\text{C}_2\text{H}_2)$ , the vinylidene  $\text{LaCCH}_2$ , the inserted  $\text{HLaCCH}$  isomers are observed on deposition, and increase on annealing. The  $\text{La}(\text{C}_2\text{H}_2)$  molecule can rearrange by 1,2-hydrogen atom migration to form the inserted  $\text{HLaCCH}$  and the vinylidene  $\text{LaCCH}_2$  isomers in the experiments. It is noteworthy that  $\text{La}_2$  dimer elongates the C–C bond to 1.355 Å in  $\text{La}_2(\text{C}_2\text{H}_2)$  as compared to the 1.346 Å C–C bond in  $\text{La}(\text{C}_2\text{H}_2)$ .

## Experimental and Theoretical Methods

The experiment for laser ablation and matrix-isolation infrared spectroscopy is similar to those previously reported.<sup>25</sup> Briefly, the Nd:YAG laser fundamental (1064 nm, 10 Hz repetition rate with 10 ns pulse width) was focused on the rotating lanthanum target. The laser-ablated La atoms were codeposited with  $\text{C}_2\text{H}_2$  (99.96%, Cambridge Isotopic Laboratories) in excess argon onto a CsI window cooled normally to 4 K by means of a closed-cycle helium refrigerator (V24SC6LSCP, Daikin Industries). Typically, a 3–10 mJ/pulse laser power was used. The isotopic  $^{13}\text{C}_2\text{H}_2$  and  $\text{C}_2\text{D}_2$  (99%, Cambridge Isotopic Laboratories) were used to prepare the  $\text{C}_2\text{H}_2/\text{Ar}$  mixtures. In general, matrix samples were deposited for 30–60 min with a typical rate of 2–4 mmol/h. After sample deposition, IR spectra were recorded on a BIO-RAD FTS-6000e spectrometer at 0.5  $\text{cm}^{-1}$  resolution using a liquid nitrogen cooled HgCdTe (MCT) detector for the spectral range of 5000–400  $\text{cm}^{-1}$ . Samples were annealed at different temperatures and subjected to broadband irradiation ( $\lambda > 250$  nm) using a high-pressure mercury arc lamp (Ushio, 100 W).

Quantum chemical calculations were performed to predict the structures and vibrational frequencies of the observed reaction products using the Gaussian 03 program.<sup>26</sup> The B3LYP density functional method was utilized.<sup>27</sup> The 6-311++G(d, p) basis set was used for H and C atoms, and SDD for La atom.<sup>28,29</sup> Geometries were fully optimized and vibrational frequencies were calculated with analytical second derivatives. Transition-state optimizations were done with the synchronous transit-guided quasi-Newton (STQN) method.

## Results and Discussion

Experiments have been done with  $\text{C}_2\text{H}_2$  concentrations ranging from 0.05% to 0.5% in excess argon. Typical infrared spectra for the reactions of laser-ablated La atoms with  $\text{C}_2\text{H}_2$  in excess argon in the selected regions are illustrated in Figures 1–3, and the absorption bands are listed in Table 1. The stepwise annealing and irradiation behaviors of these product absorptions are also shown in the figures and will be discussed below.

Quantum chemical calculations have been carried out for the possible isomers and electronic states of the potential product

\* Author to whom correspondence should be addressed. Electronic mail: q.xu@aist.go.jp.

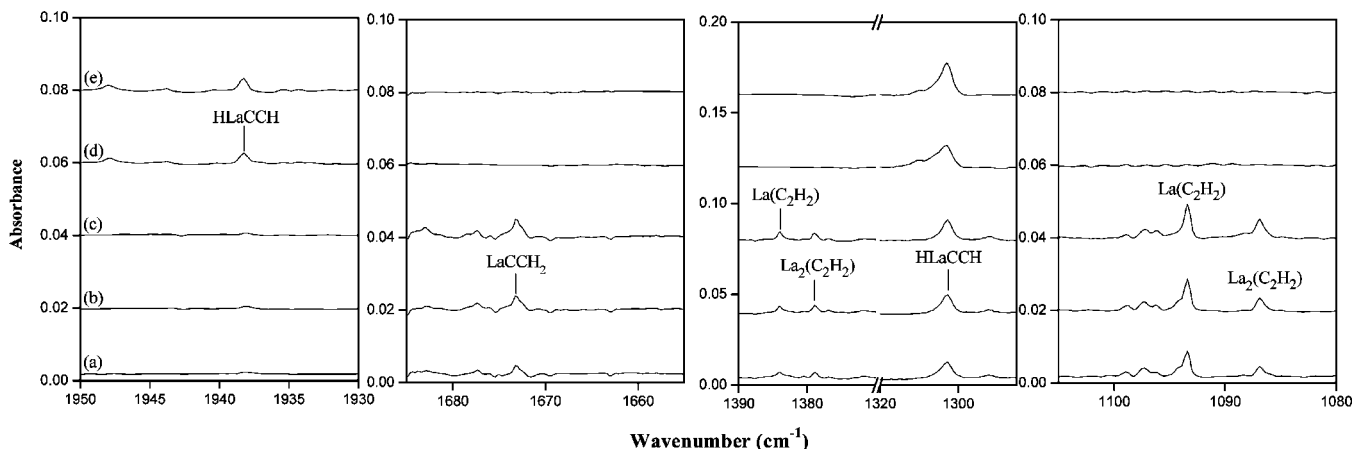


**Figure 1.** Infrared spectra in the 1950–1930, 1685–1655, 1390–1285, and 1105–1080  $\text{cm}^{-1}$  regions from codeposition of laser-ablated lanthanum atoms with 0.4%  $\text{C}_2\text{H}_2$  in argon: (a) 1 h sample deposition at 4 K; (b) after annealing to 25 K; (c) after annealing to 30 K; (d) after 15 min of broadband irradiation; (e) after annealing to 35 K.

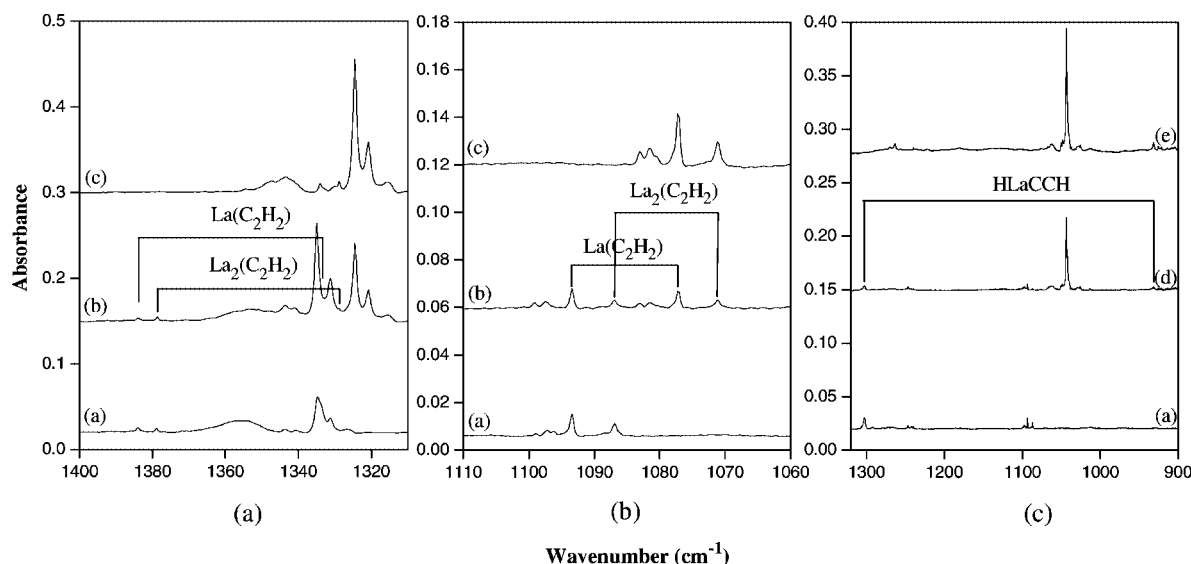


**Figure 2.** Infrared spectra in the 1400–1310, 1110–1060, and 1320–900  $\text{cm}^{-1}$  regions from codeposition of laser-ablated lanthanum atoms with  $\text{C}_2\text{H}_2$  in argon: (a) 0.4%  $^{12}\text{C}_2\text{H}_2$ ; (b) 0.2%  $^{12}\text{C}_2\text{H}_2$  + 0.2%  $^{13}\text{C}_2\text{H}_2$ ; (c) 0.4%  $^{13}\text{C}_2\text{H}_2$ ; (d) 0.2%  $^{12}\text{C}_2\text{H}_2$  + 0.2%  $^{12}\text{C}_2\text{D}_2$ ; (e) 0.4%  $^{12}\text{C}_2\text{D}_2$ .

molecules. Figure 4 shows the optimized structures and electronic ground states. Tables 2–5 report the calculated IR frequencies and isotopic frequencies of the reaction products.

**$\text{La}(\text{C}_2\text{H}_2)$ .** The absorptions at 2933.8, 1383.9, 1093.4, and 651.5  $\text{cm}^{-1}$  can be grouped together to one species, based on the growth/decay characteristics as a function of changes of experimental conditions. The four bands appear on sample deposition, visibly increase on sample annealing to 25 K, further increase on annealing to 30 K, and disappear after broadband irradiation (Table 1 and Figure 1). The 1383.9  $\text{cm}^{-1}$  band shifts to 1334.0  $\text{cm}^{-1}$  with  $^{13}\text{C}_2\text{H}_2$  and to 1349.6  $\text{cm}^{-1}$  with  $^{12}\text{C}_2\text{D}_2$ , exhibiting isotopic frequency ratios of 1.0374 ( $^{12}\text{C}_2\text{H}_2/^{13}\text{C}_2\text{H}_2$ ) and 1.0254 ( $^{12}\text{C}_2\text{H}_2/^{12}\text{C}_2\text{D}_2$ ). The  $^{12}\text{C}_2\text{H}_2/^{13}\text{C}_2\text{H}_2$  ratio indicates that the 1383.9  $\text{cm}^{-1}$  band should be assigned to a C–C stretching vibration.<sup>14</sup> As shown in Figure 2, the mixed  $^{12}\text{C}_2\text{H}_2$  +  $^{13}\text{C}_2\text{H}_2$  isotopic spectra only provide the sum of pure isotopic bands, which indicates that only one  $\text{C}_2\text{H}_2$  subunit is involved in this mode. Therefore, the 1383.9  $\text{cm}^{-1}$  band is assigned to the C–C stretching vibration of the  $\text{La}(\text{C}_2\text{H}_2)$  molecule. The C–C stretching frequency is significantly lower than that of previous reported transition metal–acetylene  $\pi$  complexes,  $\text{Ni}(\text{C}_2\text{H}_2)$  (1647  $\text{cm}^{-1}$ )<sup>7</sup> and  $\text{Cu}(\text{C}_2\text{H}_2)$  (1870  $\text{cm}^{-1}$ )<sup>4</sup> and is close to the value of metallacyclopentene,  $\text{H}_2\text{Ti}(\text{C}_2\text{H}_2)$  (1465  $\text{cm}^{-1}$ )<sup>9b</sup>

and  $\text{Cr}(\text{C}_2\text{H}_2)$  (1476  $\text{cm}^{-1}$ ),<sup>14</sup> in solid argon, indicating that  $\text{La}(\text{C}_2\text{H}_2)$  is not a  $\pi$  complex but should be considered as a metallacyclopentene. The C–C stretching vibrational frequency of  $\text{La}(\text{C}_2\text{H}_2)$  at 1383.9  $\text{cm}^{-1}$  is about 589  $\text{cm}^{-1}$  red-shifted from the C–C stretching frequency of acetylene and is about 245  $\text{cm}^{-1}$  lower than the C–C stretching frequency of ethylene.<sup>30</sup> The 2933.8, 1093.4, and 651.5  $\text{cm}^{-1}$  bands track with the 1383.9  $\text{cm}^{-1}$  band, suggesting different modes of the same molecule. The 1093.4  $\text{cm}^{-1}$  band shifts to 1077.2  $\text{cm}^{-1}$  with  $^{13}\text{C}_2\text{H}_2$  and to 921.3  $\text{cm}^{-1}$  with  $^{12}\text{C}_2\text{D}_2$  and is due to the CCH deformation mode. For this band, the mixed  $^{12}\text{C}_2\text{H}_2$  +  $^{13}\text{C}_2\text{H}_2$  (Figure 2b) and  $^{12}\text{C}_2\text{H}_2$  +  $^{13}\text{C}_2\text{D}_2$  isotopic spectra only provide the sum of pure isotopic bands, which also indicates that only one  $\text{C}_2\text{H}_2$  subunit is involved in this mode. The 2933.8  $\text{cm}^{-1}$  band shifts to 2922.6  $\text{cm}^{-1}$  with  $^{13}\text{C}_2\text{H}_2$  and to 2154.4  $\text{cm}^{-1}$  with  $^{12}\text{C}_2\text{D}_2$  and is due to the C–H stretching mode. The 651.5  $\text{cm}^{-1}$  band shifts to 644.4  $\text{cm}^{-1}$  with  $^{13}\text{C}_2\text{H}_2$  and is due to the  $\text{C}_2\text{H}_2$  tilt mode.

The assignment is strongly supported by DFT calculations. As shown in Figure 4 and Table 2, the  $\text{La}(\text{C}_2\text{H}_2)$  molecule is predicted to have an  $^2A_1$  ground state with  $C_{2v}$  symmetry (Figure 4) and is the most stable structural isomer of  $\text{La}-\text{C}_2\text{H}_2$ . The C–C stretching, CCH deformation, and  $\text{C}_2\text{H}_2$  tilt modes are

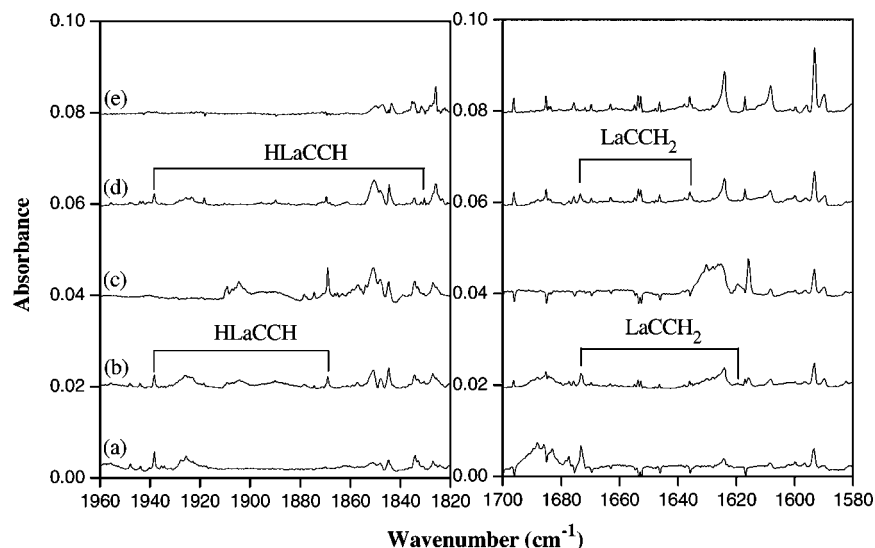


**Figure 3.** Infrared spectra in the 1960–1820 and 1700–1580  $\text{cm}^{-1}$  regions from codeposition of laser-ablated lanthanum atoms with  $\text{C}_2\text{H}_2$  in argon: (a) 0.4%  $^{12}\text{C}_2\text{H}_2$ ; (b) 0.2%  $^{12}\text{C}_2\text{H}_2$  + 0.2%  $^{13}\text{C}_2\text{H}_2$ ; (c) 0.4%  $^{13}\text{C}_2\text{H}_2$ ; (d) 0.2%  $^{12}\text{C}_2\text{H}_2$  + 0.2%  $^{12}\text{C}_2\text{D}_2$ ; (e) 0.4%  $^{12}\text{C}_2\text{D}_2$ .

**TABLE 1: Infrared Absorptions ( $\text{cm}^{-1}$ ) from Co-deposition of Laser-Ablated Lanthanum Atoms with Acetylene in Excess Argon**

$^{12}\text{C}_2\text{H}_2$	$^{13}\text{C}_2\text{H}_2$	$^{12}\text{C}_2\text{D}_2$	assignment
2933.8	2922.6	2154.4	$\text{La}(\text{C}_2\text{H}_2)$ , C–H stretching
1938.2	1869.0	1825.9	HLaCCH, C–C stretching
1673.2	1615.8	1636.0	$\text{LaCCH}_2$ , C–C stretching
1383.9	1334.0	1349.6	$\text{La}(\text{C}_2\text{H}_2)$ , C–C stretching
1378.9	1328.8	1336.8	$\text{La}_2(\text{C}_2\text{H}_2)$ , C–C stretching
1303.0	1302.9	931.8	HLaCCH, La–H stretching
1093.4	1077.2	921.3	$\text{La}(\text{C}_2\text{H}_2)$ , out-of-plane CCH deformation
1086.9	1071.2	913.8	$\text{La}_2(\text{C}_2\text{H}_2)$ , out-of-plane CCH deformation
651.5	644.4		$\text{La}(\text{C}_2\text{H}_2)$ , $\text{C}_2\text{H}_2$ tilt
559.7	557.2		$\text{La}_2(\text{C}_2\text{H}_2)$ , $\text{C}_2\text{H}_2$ torsion

calculated at 1436.2, 1115.7, and 622.9  $\text{cm}^{-1}$  (Table 2), which are in good agreement with the experimental observations (1383.9, 1093.4, and 651.5  $\text{cm}^{-1}$ ). The isotopic frequency ratios calculated for the C–C stretching and CCH deformation modes ( $^{12}\text{C}_2\text{H}_2/^{13}\text{C}_2\text{H}_2$ , 1.0385 and 1.0150;  $^{12}\text{C}_2\text{H}_2/^{12}\text{C}_2\text{D}_2$  1.0295 and 1.1971) are also consistent with the experimental observations. These agreements between the experimental and calculated vibrational frequencies, relative absorption intensities, and isotopic shifts confirm the identification of the  $\text{La}(\text{C}_2\text{H}_2)$  molecule from the matrix IR spectra.

**HLaCCH.** One set of new absorptions at 1938.2 and 1303.0  $\text{cm}^{-1}$  can be grouped together to one species, based on the growth/decay characteristics as a function of changes of experimental conditions (Table 1 and Figure 1). The two bands are assigned to the HLaCCH molecule on the basis of isotopic substitution and DFT calculations. The 1938.2  $\text{cm}^{-1}$  band shifts to 1869.0  $\text{cm}^{-1}$  with  $^{13}\text{C}_2\text{H}_2$  and to 1825.9  $\text{cm}^{-1}$  with  $^{12}\text{C}_2\text{D}_2$ , exhibiting isotopic frequency ratios of 1.0370 ( $^{12}\text{C}_2\text{H}_2/^{13}\text{C}_2\text{H}_2$ ) and 1.0615 ( $^{12}\text{C}_2\text{H}_2/^{12}\text{C}_2\text{D}_2$ ). The  $^{12}\text{C}_2\text{H}_2/^{13}\text{C}_2\text{H}_2$  ratio indicates that the 1938.2  $\text{cm}^{-1}$  band should be assigned to a C–C stretching vibration. As shown in Figure 3, in the experiments with mixed  $^{12}\text{C}_2\text{H}_2$  +  $^{13}\text{C}_2\text{H}_2$  and  $^{12}\text{C}_2\text{H}_2$  +  $^{13}\text{C}_2\text{D}_2$ , the isotopic spectra only provide the sum of pure isotopic bands, indicating that only one C–C subunit is involved in this mode. The 1303.0  $\text{cm}^{-1}$  band shows no carbon-13 shift but shifts to 931.8  $\text{cm}^{-1}$  with  $\text{C}_2\text{D}_2$  and gives an isotopic  $^{12}\text{C}_2\text{H}_2/^{12}\text{C}_2\text{D}_2$  ratio of 1.3984. The band position as well as the isotopic  $^{12}\text{C}_2\text{H}_2/^{12}\text{C}_2\text{D}_2$  ratio is close to the values of the La–H stretching vibration of various previously characterized lanthanum hydrides in excess argon,<sup>31</sup>

implying that the 1303.0  $\text{cm}^{-1}$  band is due to a La–H stretching vibration. The mixed  $^{12}\text{C}_2\text{H}_2$  +  $^{13}\text{C}_2\text{D}_2$  isotopic spectra only provide the sum of pure isotopic bands, which indicates that only one La–H subunit is involved in this mode (Figure 2c). Therefore, 1938.2 and 1303.0  $\text{cm}^{-1}$  bands are assigned to the C–C and La–H stretching vibrations of the HLaCCH molecule, respectively.

The present calculations lend support for the assignment of HLaCCH. Our calculations predict that HLaCCH has an  $^2A'$  ground state with  $C_s$  symmetry (Figure 4). The C–C and La–H stretching vibrational frequencies are calculated at 2014.4 and 1364.5  $\text{cm}^{-1}$  (Table 3), which are in agreement with the experimental observations. The calculated isotopic frequency ratios of C–C stretching mode: 1.0369 ( $^{12}\text{C}_2\text{H}_2/^{13}\text{C}_2\text{H}_2$ ) and 1.0654 ( $^{12}\text{C}_2\text{H}_2/^{12}\text{C}_2\text{D}_2$ ) fit well with the experiment values (1.0370, 1.0615). The calculated  $^{12}\text{C}_2\text{H}_2/^{12}\text{C}_2\text{D}_2$  isotopic frequency ratio (1.4037) of La–H stretching mode is also consistent with the experimental observation (1.3984). The reason that the CCH bending and C–H stretching modes are not observed in the present experiment may be due to the overlap of the excess  $\text{C}_2\text{H}_2$  absorptions. These agreements between the experimental and calculated vibrational frequencies, relative absorption intensities, and isotopic shifts confirm the identification of the HLaCCH molecule from the matrix IR spectra.

**LaCCH<sub>2</sub>.** The absorption at 1673.2  $\text{cm}^{-1}$  appears during sample deposition, visibly increases on annealing to 25 K, further increases on annealing to 30 K, and disappears after broadband irradiation (Table 1 and Figure 1). The 1673.2  $\text{cm}^{-1}$  band shifts to 1615.8  $\text{cm}^{-1}$  with  $^{13}\text{C}_2\text{H}_2$  and to 1636.0  $\text{cm}^{-1}$  with  $^{12}\text{C}_2\text{D}_2$ , exhibiting isotopic frequency ratios ( $^{12}\text{C}_2\text{H}_2/^{13}\text{C}_2\text{H}_2$ , 1.0355;  $^{12}\text{C}_2\text{H}_2/^{12}\text{C}_2\text{D}_2$ , 1.0227) characteristic of C–C stretching vibration. The mixed  $^{12}\text{C}_2\text{H}_2$  +  $^{13}\text{C}_2\text{H}_2$  and  $^{12}\text{C}_2\text{H}_2$  +  $^{12}\text{C}_2\text{D}_2$  isotopic spectra only provide the sum of pure isotopic bands (Figure 3), which indicates that only one C–C subunit is involved in this mode. The 1673.2  $\text{cm}^{-1}$  band is assigned to the C–C stretching vibration of the LaCCH<sub>2</sub> molecule.

The LaCCH<sub>2</sub> molecule is predicted to have an  $^2A_1$  electronic ground state with  $C_{2v}$  symmetry (Figure 4). At the B3LYP level of theory, the doublet LaCCH<sub>2</sub> lies 20.5 and 127.5 kcal/mol lower in energy than the quartet and sextet ones, respectively. The C–C stretching vibration for LaCCH<sub>2</sub>

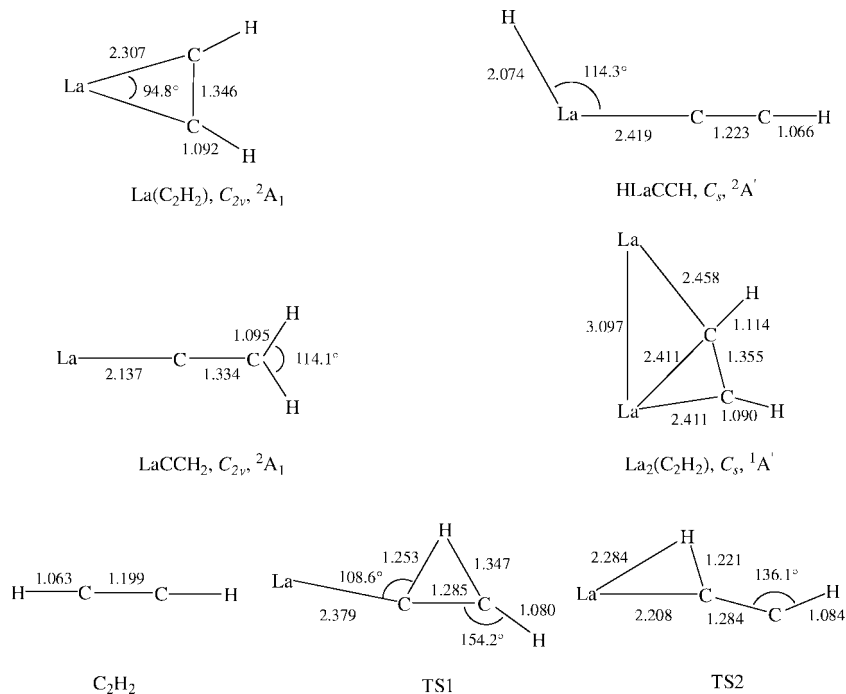


**Figure 4.** Optimized structures (bond length in Å, bond angle in degree) and electronic ground states of the possible products and transition states calculated at the B3LYP/6-311++(d,p)-SDD level.

**TABLE 2: Calculated (B3LYP/6-311++G(d,p)-SDD) Vibrational Frequencies and Intensities of  $\text{La}(\text{C}_2\text{H}_2)$  ( ${}^2A_1$ )<sup>a</sup>**

$\text{La}({}^{12}\text{C}_2\text{H}_2)$	$\text{La}({}^{13}\text{C}_2\text{H}_2)$	$\text{La}({}^{12}\text{C}_2\text{D}_2)$	mode
3083.2 (66)	3072.1 (68)	2301.8 (18)	symm C–H stretching
3052.1 (34)	3043.3 (34)	2247.8 (14)	antisymm C–H stretching
1436.2 (14)	1383.0 (12)	1395.0 (15)	C–C stretching
1115.7 (41)	1099.2 (42)	932.0 (15)	in-plane CCH deformation
984.6 (0)	975.2 (0)	779.0 (0)	$\text{C}_2\text{H}_2$ torsion
831.8 (12)	830.9 (13)	598.7 (1)	in-plane CCH deformation
622.9 (66)	619.5 (64)	483.8 (65)	$\text{C}_2\text{H}_2$ tilt
498.2 (64)	482.7 (60)	472.2 (44)	symm La–C stretching
471.3 (42)	458.5 (39)	414.8 (39)	antisymm La–C stretching

<sup>a</sup> Vibrational frequencies are given in reciprocal centimeters; intensities (in parentheses) are given in kilometers per mole.

**TABLE 3: Calculated (B3LYP/6-311++G(d,p)-SDD) Vibrational Frequencies and Intensities of  $\text{HLaCCH}$  ( ${}^2A_1$ )<sup>a</sup>**

HLaCCH	$\text{HLa}^{13}\text{C}^{13}\text{CH}$	$\text{DLaCCD}$	mode
3438.1 (26)	3432.3 (27)	2655.0 (2)	C–H stretching
2014.4 (74)	1942.7 (67)	1890.7 (87)	C–C stretching
1364.5 (719)	1369.8 (725)	972.1 (367)	La–H stretching
734.9 (49)	730.0 (50)	583.1 (22)	out-of-plane CCH bending
724.5 (45)	719.6 (46)	575.2 (19)	in-plane CCH bending

<sup>a</sup> Vibrational frequencies are given in reciprocal centimeters; intensities (in parentheses) are given in kilometers per mole.

is calculated at  $1619.3\text{ cm}^{-1}$  (Table 4), which is in reasonable agreement with the experimental observations ( $1673.2\text{ cm}^{-1}$ ). Furthermore, the calculated  ${}^{12}\text{C}_2\text{H}_2/{}^{13}\text{C}_2\text{H}_2$  and  ${}^{12}\text{C}_2\text{H}_2/{}^{12}\text{C}_2\text{D}_2$  isotopic frequency ratios (1.0345 and 1.0272) for the C–C stretching mode are also consistent with the experimental values.

**$\text{La}_2(\text{C}_2\text{H}_2)$ .** The absorptions at 1378.9, 1086.9, and  $559.7\text{ cm}^{-1}$  appear during sample deposition, visibly increase on annealing to 25 K, slightly increase on further annealing to 30 K, disappear after broadband irradiation (Table 1 and Figure 1). The  $1378.9\text{ cm}^{-1}$  band shifts to  $1328.8\text{ cm}^{-1}$  with  ${}^{13}\text{C}_2\text{H}_2$  and to  $1336.8\text{ cm}^{-1}$  with  ${}^{12}\text{C}_2\text{D}_2$ , exhibiting isotopic frequency ratios ( ${}^{12}\text{C}_2\text{H}_2/{}^{13}\text{C}_2\text{H}_2$ , 1.0377;  ${}^{12}\text{C}_2\text{H}_2/{}^{12}\text{C}_2\text{D}_2$ , 1.0315) charac-

**TABLE 4: Calculated (B3LYP/6-311++G(d,p)-SDD) Vibrational Frequencies and Intensities of  $\text{LaCCH}_2$  ( ${}^2A_1$ )<sup>a</sup>**

$\text{LaCCH}_2$	$\text{La}^{13}\text{C}^{13}\text{CH}_2$	$\text{LaCCD}_2$	mode
3048.0 (26)	3036.0 (25)	2273.0 (19)	antisymm C–H stretching
3006.3 (148)	3001.0 (147)	2196.3 (92)	symm C–H stretching
1619.3 (52)	1565.3 (48)	1576.0 (37)	C–C stretching
1418.5 (0.5)	1407.4 (2)	1052.8 (1)	H–C–H scissoring
1006.8 (12)	995.7 (11)	804.1 (19)	H–C–H rocking
965.3 (32)	955.1 (32)	772.3 (17)	out-of-plane CCH deformation
443.7 (57)	430.3 (53)	426.2 (53)	La–C stretching

<sup>a</sup> Vibrational frequencies are given in reciprocal centimeters; intensities (in parentheses) are given in kilometers per mole.

**TABLE 5: Calculated (B3LYP/6-311++G(d,p)-SDD) Vibrational Frequencies and Intensities of  $\text{La}_2(\text{C}_2\text{H}_2)$  ( ${}^1A'$ )<sup>a</sup>**

$\text{La}_2(\text{C}_2\text{H}_2)$	$\text{La}_2({}^{13}\text{C}_2\text{H}_2)$	$\text{La}_2(\text{C}_2\text{D}_2)$	mode
3101.9 (24)	3091.8 (26)	2301.0 (2)	C–H stretching
2824.2 (7)	2815.6 (7)	2087.1 (0.3)	C–H stretching
1368.0 (155)	1317.5 (140)	1332.0 (165)	C–C stretching
1130.7 (19)	1115.8 (20)	930.6 (7)	in-plane CCH deformation
869.7 (0.4)	861.8 (0.5)	688.7 (0)	$\text{C}_2\text{H}_2$ torsion
819.8 (45)	818.3 (47)	592.2 (17)	in-plane CCH deformation
526.0 (97)	523.1 (95)	432.8 (12)	$\text{C}_2\text{H}_2$ torsion
477.6 (14)	463.4 (13)	399.5 (62)	La–C stretching
400.5 (4)	388.3 (3)	388.4 (4)	La–C stretching

<sup>a</sup> Vibrational frequencies are given in reciprocal centimeters; intensities (in parentheses) are given in kilometers per mole.

teristic of C–C stretching vibration. As shown in Figure 2, the mixed  ${}^{12}\text{C}_2\text{H}_2 + {}^{13}\text{C}_2\text{H}_2$  isotopic spectra only provide the sum of pure isotopic bands, which indicates that only one  $\text{C}_2\text{H}_2$  subunit is involved in this mode. The  $1086.9\text{ cm}^{-1}$  band, which is due to the CCH deformation mode, shifts to  $1071.2\text{ cm}^{-1}$  with  ${}^{13}\text{C}_2\text{H}_2$  and to  $913.8\text{ cm}^{-1}$  with  ${}^{12}\text{C}_2\text{D}_2$ . The  $559.7\text{ cm}^{-1}$  band, which is due to the  $\text{C}_2\text{H}_2$  torsion mode, shifts to  $557.2\text{ cm}^{-1}$  with  ${}^{13}\text{C}_2\text{H}_2$ . In addition, the three bands are favored with larger laser energy, indicating more than one La atoms are involved. The three bands are therefore assigned to the  $\text{La}_2(\text{C}_2\text{H}_2)$  molecule.

$\text{La}_2(\text{C}_2\text{H}_2)$  is predicted to have an  ${}^1A'$  ground state with  $C_s$  symmetry, lying 11.6 and 12.1 kcal/mol lower in energy than

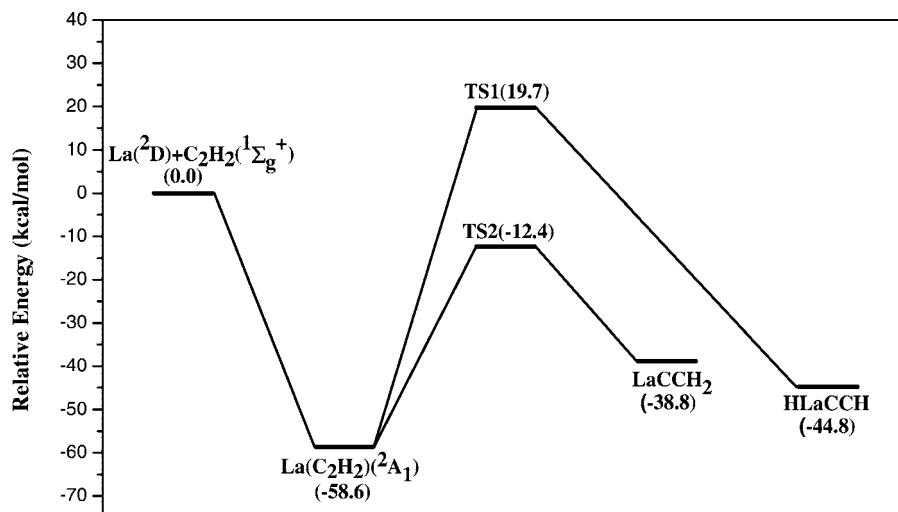
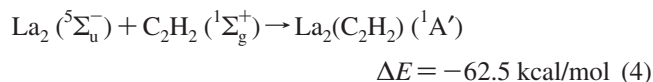
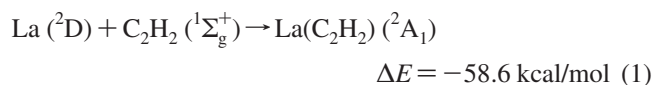


**Figure 5.** Potential energy surface for the La + C<sub>2</sub>H<sub>2</sub> reactions calculated at the B3LYP/6-311++(d,p)-SDD level. Energies given are in kcal/mol and are relative to the separated ground-state reactants: La(<sup>2</sup>D) + C<sub>2</sub>H<sub>2</sub>(<sup>1</sup>μ<sub>g</sub><sup>+</sup>).

the triplet and quintet ones, respectively, at the B3LYP level of theory (Figure 4), which is different from the reported stable Pd<sub>2</sub>(C<sub>2</sub>H<sub>2</sub>) molecule that was predicted to have a C<sub>2v</sub> symmetry.<sup>16</sup> As shown in Figure 4, La<sub>2</sub> dimer elongates the C–C bond to 1.355 Å in La<sub>2</sub>(C<sub>2</sub>H<sub>2</sub>) as compared to the 1.346 Å C–C bond in La(C<sub>2</sub>H<sub>2</sub>). The C–C stretching, CCH deformation and C<sub>2</sub>H<sub>2</sub> torsion vibrational frequencies of La<sub>2</sub>(C<sub>2</sub>H<sub>2</sub>) are calculated at 1368.0, 1130.7, and 526.0 cm<sup>-1</sup> (Table 5), which are in accord with our observed values 1378.9, 1086.0, and 559.7 cm<sup>-1</sup>. For the 1368.0 cm<sup>-1</sup> band, the calculated <sup>12</sup>C<sub>2</sub>H<sub>2</sub>/<sup>13</sup>C<sub>2</sub>H<sub>2</sub> and <sup>12</sup>C<sub>2</sub>H<sub>2</sub>/<sup>12</sup>C<sub>2</sub>D<sub>2</sub> isotopic frequency ratios (1.0383 and 1.0270) are consistent with the experimental observations (1.0377 and 1.0315). For the 1130.7 cm<sup>-1</sup> band, the calculated <sup>12</sup>C<sub>2</sub>H<sub>2</sub>/<sup>13</sup>C<sub>2</sub>H<sub>2</sub> and <sup>12</sup>C<sub>2</sub>H<sub>2</sub>/<sup>12</sup>C<sub>2</sub>D<sub>2</sub> isotopic frequency ratios (1.0134 and 1.2150) are also consistent with the experimental observations. The assignment of the La<sub>2</sub>(C<sub>2</sub>H<sub>2</sub>) molecule is supported by these agreements between the experimental and calculated vibrational frequencies, relative absorption intensities, and isotopic shifts.

**Reaction Mechanism.** Laser-ablated La atoms react with C<sub>2</sub>H<sub>2</sub> to form three isomers, La(C<sub>2</sub>H<sub>2</sub>), HLaCCH, and LaCCH<sub>2</sub> during sample deposition, which visibly increase on annealing (Figure 1). According to reactions 1–3, the reactions are predicted to be exothermic by 58.6, 44.8, and 38.8 kcal/mol, respectively. The La(C<sub>2</sub>H<sub>2</sub>) and LaCCH<sub>2</sub> molecule disappear, whereas the HLaCCH molecule increases after broadband irradiation, indicating rearrangement reactions take place during broadband irradiation. To have a better understanding of the rearrangement reactions, potential energy surfaces starting from La + C<sub>2</sub>H<sub>2</sub> are calculated at the level of B3LYP, as shown in Figure 5. The ground-state <sup>2</sup>D lanthanum atoms react with acetylene to form an <sup>2</sup>A<sub>1</sub> state La(C<sub>2</sub>H<sub>2</sub>) molecule; the reaction is predicted to be exothermic by about 58.6 kcal/mol with minimal activation energy. Two transition states have been located on the potential energy surfaces, which connect the equilibrium structure of La(C<sub>2</sub>H<sub>2</sub>) with HLaCCH and LaCCH<sub>2</sub>. The optimized transition-state structures are shown in Figure 4. Therefore, plausible reaction mechanisms can be proposed as follows on the basis of the behavior of sample annealing and irradiation together with the observed species and calculated stable isomers. The La atoms initially interact with the C–C triple bond of the C<sub>2</sub>H<sub>2</sub> forming the La(C<sub>2</sub>H<sub>2</sub>) complex. La(C<sub>2</sub>H<sub>2</sub>) rearranges to HLaCCH with a barrier of 78.3 kcal/mol (Figure 5), which can be obtained by broadband irradiation.

The CCH radicals are observed after the broadband irradiation (1844.8 cm<sup>-1</sup>),<sup>15,16</sup> indicating that part of HLaCCH products are decomposed to H, La, and CCH upon the broadband irradiation. LaCCH<sub>2</sub> is observed after deposition and the predicted isomerization barrier from La(C<sub>2</sub>H<sub>2</sub>) to LaCCH<sub>2</sub> lies below the energy of La + C<sub>2</sub>H<sub>2</sub> (Figures 1 and 5), suggesting that laser-ablated La atoms can also react with C<sub>2</sub>H<sub>2</sub> to form LaCCH<sub>2</sub> directly. It can be seen from Figure 1 that the IR absorptions of La<sub>2</sub>(C<sub>2</sub>H<sub>2</sub>) appear during sample deposition, visibly increase on annealing, suggesting that the La<sub>2</sub> dimer can react with acetylene molecules to form the La<sub>2</sub>(C<sub>2</sub>H<sub>2</sub>) molecule spontaneously according to reactions 4, which is predicted to be exothermic by 62.5 kcal/mol.



## Conclusions

Reactions of laser-ablated La atoms with acetylene in excess argon have been studied using matrix-isolation infrared spectroscopy. On the basis of the isotopic shifts and splitting patterns, the La(C<sub>2</sub>H<sub>2</sub>), LaCCH<sub>2</sub>, HLaCCH, and La<sub>2</sub>(C<sub>2</sub>H<sub>2</sub>) molecules have been characterized. Density functional theory calculations have been performed, which lend strong support to the experimental assignments of the infrared spectra. In addition, the plausible reaction mechanism for the formation of the products has been proposed.

**Acknowledgment.** We thank the reviewers for their valuable comments and suggestions. This work was supported by a Grant-in-Aid for Scientific Research (B) (Grant No. 17350012) from the Ministry of Education, Culture, Sports, Science and Technology (MEXT) of Japan. Y.-L.T. thanks JASSO and Kobe University for Honors Scholarship.

## References and Notes

- (1) Rashidi, M.; Puddephatt, R. J. *J. Am. Chem. Soc.* **1986**, *108*, 7111.
- (2) Cremer, P. S.; Su, S. D.; Shen, Y. R.; Somorjai, G. A. *J. Phys. Chem. B* **1997**, *101*, 6474.
- (3) Kose, R.; Brown, W. A.; King, D. A. *J. Am. Chem. Soc.* **1999**, *121*, 4845.
- (4) Ozin, G. A.; McIntosh, D. F.; Power, W. J.; Messmer, R. P. *Inorg. Chem.* **1981**, *20*, 1782.
- (5) Kasai, P. H. *J. Am. Chem. Soc.* **1982**, *104*, 1165.
- (6) Kasai, P. H. *J. Am. Chem. Soc.* **1992**, *114*, 3299.
- (7) Kline, E. S.; Kafafi, Z. H.; Hauge, R. H.; Margrave, J. L. *J. Am. Chem. Soc.* **1987**, *109*, 2402.
- (8) (a) Burkholder, T. R.; Andrews, L. *Inorg. Chem.* **1993**, *3* (2), 2491. (b) Chertihin, G. V.; Andrews, L. *J. Am. Chem. Soc.* **1994**, *116*, 3513.
- (9) (a) Manceron, L.; Andrews, L. *J. Am. Chem. Soc.* **1985**, *107*, 563. (b) Lee, Y. K.; Manceron, L.; Papai, I. *J. Phys. Chem. A* **1997**, *101*, 9650.
- (10) Andrews, L.; Hassanzadeh, P.; Martin, J. M. L.; Taylor, P. R. *J. Phys. Chem.* **1993**, *97*, 5839.
- (11) Thompson, C. A.; Andrews, L. *J. Am. Chem. Soc.* **1996**, *118*, 10242.
- (12) Kline, E. S.; Kafafi, Z. H.; Hauge, R. H.; Margrave, J. L. *J. Am. Chem. Soc.* **1985**, *107*, 7559.
- (13) Chenier, J. H. B.; Howard, J. A.; Mile, B.; Sutcliffe, R. *J. Am. Chem. Soc.* **1983**, *105*, 788.
- (14) Huang, Z. G.; Zeng, A. H.; Dong, J.; Zhou, M. F. *J. Phys. Chem. A* **2003**, *107*, 2329.
- (15) Wang, X. F.; Andrew, L. *J. Phys. Chem. A* **2004**, *108*, 4838.
- (16) Wang, X. F.; Andrew, L. *J. Phys. Chem. A* **2003**, *107*, 337.
- (17) Andrew, L.; Kushto, G. P.; Marsden, C. *J. Chem. Eur. J.* **2006**, *12*, 8324.
- (18) Cohen, D.; Basch, H. *J. Am. Chem. Soc.* **1983**, *105*, 6980.
- (19) Sodupe, M.; Bauschlicher, C. W. *J. Phys. Chem.* **1991**, *95*, 8640.
- (20) Bauschlicher, C. W.; Langhoff, S. R. *J. Phys. Chem.* **1991**, *95*, 2278.
- (21) Rosi, M.; Bauschlicher, C. W. *Chem. Phys. Lett.* **1990**, *166*, 189.
- (22) Fournier, R. *Int. J. Quantum Chem.* **1994**, *52*, 973.
- (23) Bohme, M.; Wagener, T.; Frenking, G. *J. Organomet. Chem.* **1996**, *520*, 31.
- (24) (a) Zhou, M. F.; Andrews, L.; Bauschlicher, C. W., Jr. *Chem. Rev.* **2001**, *101*, 1931. (b) Himmel, H. J.; Downs, A. J.; Greene, T. M. *Chem. Rev.* **2002**, *102*, 4191, and references therein.
- (25) (a) Burkholder, T. R.; Andrews, L. *J. Chem. Phys.* **1991**, *95*, 8697. (b) Zhou, M. F.; Tsumori, N.; Andrews, L.; Xu, Q. *J. Phys. Chem. A* **2003**, *107*, 2458. (c) Xu, Q.; Jiang, L.; Tsumori, N. *Angew. Chem., Int. Ed.* **2005**, *44*, 4338. (d) Jiang, L.; Xu, Q. *J. Am. Chem. Soc.* **2005**, *127*, 42. (e) Jiang, L.; Xu, Q. *J. Am. Chem. Soc.* **2005**, *127*, 8906.
- (26) Frisch, M. J.; Trucks, G. W.; Schlegel, H. B.; Scuseria, G. E.; Robb, M. A.; Cheeseman, J. R.; Montgomery, J. A., Jr.; Vreven, T.; Kudin, K. N.; Burant, J. C.; Millam, J. M.; Iyengar, S. S.; Tomasi, J.; Barone, V.; Mennucci, B.; Cossi, M.; Scalmani, G.; Rega, N.; Petersson, G. A.; Nakatsuji, H.; Hada, M.; Ehara, M.; Toyota, K.; Fukuda, R.; Hasegawa, J.; Ishida, M.; Nakajima, T.; Honda, Y.; Kitao, O.; Nakai, H.; Klene, M.; Li, X.; Knox, J. E.; Hratchian, H. P.; Cross, J. B.; Adamo, C.; Jaramillo, J.; Gomperts, R.; Stratmann, R. E.; Yazyev, O.; Austin, A. J.; Cammi, R.; Pomelli, C.; Ochterski, J. W.; Ayala, P. Y.; Morokuma, K.; Voth, G. A.; Salvador, P.; Dannenberg, J. J.; Zakrzewski, V. G.; Dapprich, S.; Daniels, A. D.; Strain, M. C.; Farkas, O.; Malick, D. K.; Rabuck, A. D.; Raghavachari, K.; Foresman, J. B.; Ortiz, J. V.; Cui, Q.; Baboul, A. G.; Clifford, S.; Cioslowski, J.; Stefanov, B. B.; Liu, G.; Liashenko, A.; Piskorz, P.; Komaromi, I.; Martin, R. L.; Fox, D. J.; Keith, T.; Al-Laham, M. A.; Peng, C. Y.; Nanayakkara, A.; Challacombe, M.; Gill, P. M. W.; Johnson, B.; Chen, W.; Wong, M. W.; Gonzalez, C.; Pople, J. A. *Gaussian 03*, revision B.04; Gaussian, Inc.: Pittsburgh, PA, 2003.
- (27) (a) Lee, C.; Yang, E.; Parr, R. G. *Phys. Rev. B* **1988**, *37*, 785. (b) Becke, A. D. *J. Chem. Phys.* **1993**, *98*, 5648.
- (28) (a) Krishnan, R.; Binkley, J. S.; Seeger, R.; Pople, J. A. *J. Chem. Phys.* **1980**, *72*, 650. (b) Frisch, M. J.; Pople, J. A.; Binkley, J. S. *J. Chem. Phys.* **1984**, *80*, 3265.
- (29) Dolg, M.; Stoll, H.; Preuss, H. *J. Chem. Phys.* **1989**, *90*, 1730.
- (30) Cowieson, D. R.; Barnes, A. J.; Orville-Thomas, W. J. *J. Raman Spectrosc.* **1981**, *10*, 224.
- (31) Wang, X. F.; Chertihin, G. V.; Andrew, L. *J. Phys. Chem. A* **2002**, *106*, 9213.